No. 68-1036

TEST AND ANALYSIS OF GRAPHITE-FIBER, EPOXY-RESIN COMPOSITE AIRFRAME STRUCTURAL ELEMENTS

by

K. H. SAYERS and D. P. HANLEY
Bell Aerosystems Company
Buffalo, New York

AIAA Paper
No. 68-1036

AIAA 5th Annual Meeting and Technical Display

PHILADELPHIA, PENNSYLVANIA/OCTOBER 21-24, 1968

DISCLAIMER NOTICE

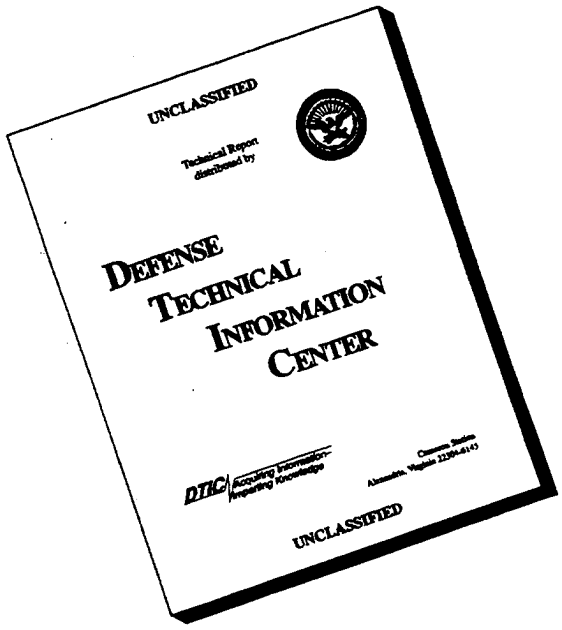

THIS DOCUMENT IS BEST QUALITY AVAILABLE. THE COPY FURNISHED TO DTIC CONTAINED A SIGNIFICANT NUMBER OF PAGES WHICH DO NOT REPRODUCE LEGIBLY.

TEST AND ANALYSIS OF GRAPHITE - FIBER, EPOXY - RESIN COMPOSITE AIRFRAME STRUCTURAL ELEMENTS*

K.H. SAYERS, Senior Structures Engineer and
D.P. HANLEY, Chief, Composite Structures

Bell Aerosystems Company, A Textron Co.
Buffalo, New York

ABSTRACT

A series of graphite fiber composite stiffened panels was tested in compression and shear to select the best design for a representative fuselage component. A curved composite stiffened panel and two aluminum panels were also tested in compression. Conventional laboratory equipment and testing techniques were employed. Analytical predictions of behavior were obtained using recently developed methods. Initial buckling data, overall panel stiffnesses, ultimate strengths and failure modes were obtained. These data correlated well with theoretical predictions. An applicable post-buckling analysis for composite stiffened panels is required. A material strength problem was exposed which was subsequently solved, in part, through the use of treated fiber. Substantial strength-weight and high stiffness-weight performances were demonstrated in comparison with conventional materials.

NOMENCLATURE

a Length of buckled skin between potted ends.

A Cross sectional area of stringer.

b Width of buckled skin between stringer flats.

b' Total width of compression panel skin.

D Flexural stiffnesses.

E Young's Modulus.

G In-plane shear stiffness.

L Overall length of compression panel.

m Number of axial half-waves.

M Moments per unit width of plate.

N Loads per unit width of plate (or panel).

P Total load on stiffened panel.

t Skin thickness.

W Weight per unit area.

δ Axial deflection of compression panel.

ϵ Strains in a plate.

K Curvatures of a plate.

ρ Density.

σ Stress.

$\bar{\sigma}$ Ultimate Strength.

Subscripts

AV	Average	S	Stringer
CR	Critical loading	X	Axial loading
EQ	Equivalent	XY	Shear loading
P	Skin		

INTRODUCTION

The high specific strengths and stiffnesses available[1,4,6] with graphite fiber composites, combined with superior fatigue characteristics[2] have prompted application studies[3,5] for primary airframe structures. A structure showing high potential payoff is the stiffened shell which benefits significantly from materials of high stiffness and low density. In aircraft fuselage shell construction weight savings of 35% to 50% have been predicted[1,3] for graphite fiber composites over conventional metals. Stiffened shell elements such as stringers, plates, and skin-stringer combinations are subjected to compressive and shear loads which demand consideration of their buckling and ultimate strengths in light-to-moderate loading ranges[5].

This paper presents work undertaken as part of a program[6] concerned with an integrated approach to research on and design methods for graphite composite materials. In this program a representative fuselage component has been designed and fabricated and it will be evaluated later in order to demonstrate the potential advantages of the graphite composite material and to permit correlation of analytically predicted and measured performance. The testing and analysis work reported herein permitted selection of the final shell design and established confidence in the design techniques used. The advantages of graphite composite construction were demonstrated and a number of areas requiring future research work were defined.

DESIGN REQUIREMENTS

The load requirements for the representative fuselage component are as follows:

Direct loading (due to bending and/or axial load)
Ultimate: $N_x = \pm 1{,}800$ lb/in.
Limit: $N_x = \pm 1{,}200$ lb/in.
Shear loading (due to torsion and/or shear force)
Ultimate: $N_{xy} = \pm 180$ lb/in.
Limit: $N_{xy} = \pm 120$ lb/in.

It is required that there be no permanent structural deformation below limit load. As little was known of the post buckling behavior of composite structures when the design criteria were established, initial buckling of plate elements below limit load was to be avoided. Catastrophic failure must not occur below the ultimate load requirement.

The above requirements must be met with the lowest practical shell weight and sufficient stiffness must be provided. The panel tests were evaluated in terms of these requirements. Extrapolation from the shell requirements was considered possible since only small curvature and load redistribution effects are anticipated in the shell static test. These are usually beneficial effects with respect to the ultimate strength attained.

* *The work reported herein was supported in part by the Advanced Research Projects Agency, Department of Defense, through the Air Force Materials Laboratory under Contract AF 33(615)-3110.*

TEST PANELS

A series of composite stiffened panels was designed and fabricated. The constructions listed (Tables 1 and 2) were chosen after extensive analytical investigation as being likely to satisfy design requirements. The purpose of the tests was to select the best candidate for use in the shell construction. Panels 1 through 9 were made by Union Carbide Corporation, Carbon Products Division. Panels 10 through 12, subsequently discussed, were made by Bell Aerosystems.

Compression Panels

The compression panels were made to the design shown in Figure 1 using Thornel† 40 (Panels 1 through 4) and Thornel 50 (Panel 5) and ERL 2256/MPDA epoxy resin. The properties achieved are shown in Table 1. The fiber contents (Panels 2 through 5) account for measured void contents which were in the range 4-5%. Void contents were not measured for Panel 1.

Panel 10 was sectioned from a Bell manufacturing technology demonstration component. This structure was 6-inches in diameter and 12-inches long. The cylinder skin featured two quadrants having (0, ±10, 0^{o}) layups as shown in Figure 2 and two quadrants having ($\pm 45^{o}$) layups. This method of construction is considered representative of tailored composite fuselage construction wherein bending and shear strengths are provided efficiently. The Thornel 40 skin and stringers of the test panel had an estimated fiber content of 50%. The stringers were cut to allow for insertion of Thornel 50 stiffening rings (Figures 2 and 3).

Panels 11 and 12 were made of 7075-T6 aluminum. They were of the same basic design as the flat composite panels (Figure 1), but had 0.040-inch skins and 0.032-inch stringers. These panels provided some direct, although limited, comparative data for evaluating the composite panel test results. The weight/unit area of the aluminum panels was about twice that of the composite panels.

All the compression panels were successfully tested using potted ends (Figures 3 and 4). The potting compound used was Epon 828/Versamid 140/diethylene triamine/$CaCO_3$ inert filler in weight proportions of 100/15/8/50. The calcium carbonate filler was added to reduce resin shrinkage which had caused slight panel curvature during earlier panel tests on another project. After careful centering with respect to computed neutral axes and overnight cure at room temperature (one end at a time), the potted end faces were ground flat and parallel to within 0.001-inch TIR.

Shear Panels

The shear panels were made to the design shown in Figure 5. Thornel 40 was used in Panels 6 through 8 and Thornel 50 in Panel 9. The properties of these panels are shown in Table 2. Fiber contents listed (Panels 7 through 9) in Table 2 account for the measured void contents which were in the range 1-4%. Void contents were not measured for Panel 6.

The shear panels were tested in an articulated picture-frame fixture (Figure 6) using a special edge attachment technique (Figure 5). The edges of the composite panel were bonded between aluminum doubler plates using 1-inch wide AF 126 Scotchweld adhesive. Doublers were bolted to the steel frame using appropriate shimming. The corners of the composite panels incorporated diagonal 0.1-inch wide cuts ending in 0.25-inch diameter holes to provide local strain relief (Figures 6 and 12).

EXPERIMENTAL RESULTS

Compression Panels

The test setup shown in Figure 4 employed two dial gages to monitor ram movement. On panels 1 through 5 (16-inch lengths), ten strain gages were provided to detect panel bending and initial skin buckling. Dial gages mounted horizontally showed that panel bending was slight in all cases. The panels were loaded in 500 lb increments, gage readings being taken during load-holds. The composite panels (No's. 1 through 5 and 10) failed suddenly and catastrophically. Failure of the aluminum panels (No's. 11 and 12) was more gradual and resulted in permanent plastic deformations. Panels 1 through 4 failed such that it was possible to machine off the failed ends, re-pot and re-test them. This was repeated a second time (Panels 1 and 2) when enough of the retested specimen remained undamaged.

The overall stiffnesses of the flat composite panels are given in Table 3. Stiffnesses of the curved composite panel and the aluminum panels are given in Tables 7 and 8. The measured initial stiffnesses were obtained from the dial gage data. Correlation with stiffnesses obtained from strain gage data was very good (within 4%) for the full-length panels (Nos. 1 through 5). A typical load-deflection curve is given in Figure 7.

The average initial buckling strains and the observed buckling modes are given in Tables 4 and 8. Onset of initial buckling was detected visually and from strain gage data where available (see typical example, Figure 8). No initial buckling was observed during the curved panel test. The different modes obtained with different skin types are worthy of note (for instance, the dependency of buckle mode patterns on skin orientation, Table 4, Panels 1 and 2). All modes were symmetrical with respect to the central stringer and remained stable.

Ultimate and initial buckling strengths of the flat composite panels are given in Table 5. All of these panels met the ultimate requirement, while four of the five panels were marginal with respect to the limit design strength requirement. This latter condition was believed due to the skins being thinner than desired. No definite trend was observed in the panel ultimate strengths for the several lengths tested, although the failure loads and modes strongly suggest a material compression strength cutoff, i.e., lack of column action. The third test of Panel 1 appears anomolously high but this may be accounted for by the somewhat greater thicknesses at the one end that were preserved during the retests.

Stringer stresses at failure were estimated from measured strains and computed moduli reduced appropriately to account for equilibrium requirements. These stresses, in the case of Panels 1 through 4, indicated a basic material and/or process deficiency. Material compression strengths of 44,000 and 54,000 psi were previously attained (Reference 6, Part II, Table XLIV) on (90, 0, 0, 90^{o}) and ($\pm 10, \mp 10^{o}$) Thornel 40 laminates whereas the estimated strengths achieved by the stringers were only about half these values (Table 5). The stringer strengths were confirmed in some cases by separate compression tests on short specimens cut from the ends of the panel stringers prior to assembly. Panel 5 was made of treated Thornel 50 and this was partially successful in resolving the strength problem as evidenced by the considerable increase in panel ultimate strength and estimated stringer failure stress. Reasons for the material strength deficiency with untreated Thornel 40 are currently being investigated, in particular the effect of void content. Improved fiber treatments are also being studied.

The ultimate strength of the curved panel is given in Table 7a. Achieved strength is low since failure occurred prematurely, starting at the stringer cutouts. Separate tests on short unnotched stringer sections yielded ultimate stresses (72 to 91.2 ksi, refer Table 7b) about three times those estimated from the panel test (28 ksi, refer Table 7a). Thus is shown both the importance of providing proper cutout reinforcements in composite structures and the high potential strengths obtainable.

Ultimate strengths of the aluminum panels are given in Table 8. Failure was by stringer crippling at an average stringer stress of 62,500 psi, slightly below the material compressive yield strength.

Shear Panels

The shear panel test setup is shown in Figure 6. On the first panel tested (Panel 6), four strain gage rosettes were located diagonally across the panel in line with the load. In addition, four gages were mounted to detect stringer bending. Following the first test, most of these gages were judged to be superfluous as they gave very low readings and subsequently only gages mounted on the loaded diagonal were used.

Panels were loaded in increments of 200 or 250 lb with strain readings being taken during load-holds. Initial skin buckling was neither expected or observed during these tests. Strain data showed that shear strains were reasonably constant over the panel surfaces, Figure 11 shows a typical result. Proportional limits and ultimate strengths are given in Table 6. The proportional limit load corresponded to either a departure from linearity of the load-strain curve or the occurrence of panel damage (cracks, etc.). Ultimate strengths

† *Thornel is a trademark of the Union Carbide Corp. for graphite yarn.*

corresponded to panel failures and were characterized in all cases by large cracks initiating at the corners and spreading along the panel edges (Figure 13).

Creep was observed during the test of Panel 6 (See Figure 11) but not in the other shear panel tests. This confirms earlier suspicions of room-temperature creep and suggests that viscoelastic loading rate effects may be significant in testing some types of laminates. Figure 12 shows the failure of Panel 6. Stringers remained bonded during tests of Panels 7 through 9, possibly due to the smaller skin shear strains experienced. Panel shear stiffnesses deduced from tests are given in Table 6. With respect to the loading requirements, all panels exceeded both the limit and ultimate requirements, with the exception of Panel 6 which was marginal on limit load. Localized damage unavoidably occurred due to the corner 'keyholes'. Better performance is expected in the 'discontinuity free' fuselage test structure. Although the standard test technique used was adequate in obtaining the shear stiffnesses of graphite composite panels, it did yield conservative values of shear strength.

Failure Modes

The shear panel failure modes were localized and not representative of gross failure. Compression panel failures were all similar in that fractures ran from side-to-side of the specimens and involved both skin and stringers. It was not possible to identify where failures began since they were sudden and catastrophic; it was possible to separate the panels by hand into two pieces after test (Figure 10).

Three types of local failure were observed: (a) laminates with 0^o outside layers (Figures 9 and 14), where small transverse folds in the surface fibers were observed accompanied by some longitudinal splitting; (b) laminates with 90^o outside layers (Figure 9), where massive transverse surface splitting occurred with damage to inside layers (including the 'fold' mode when the latter were 0^o layers); (c) laminates with 10^o outside layers (Figure 15), where folds in the surface fibers occurred along with long splits parallel to the fibers (Figure 10).

CORRELATION WITH THEORY

Compression Panels

The panels consisted of thin plates reinforced by stringers of symmetrical cross-section. Loads were assumed applied with no eccentricity and the stresses were assumed to remain in the elastic range. Euler-type column failure was not considered as none of the panels failed in this mode. Computed elastic constants based on measured fiber contents and thicknesses were used in the theoretical predictions.

Consideration of equilibrium gives

$$P = b't\ \sigma_p + 3A_s\ \sigma_s \tag{1}$$

Applying the constant-strain condition

$$\epsilon = \frac{\sigma_p}{Ep} = \frac{\sigma_s}{E_s} \tag{2}$$

Combining equations (1) and (2) results in

$$\sigma_p = P \Big/ \left\{ t\,b' + 3A_s \frac{Es}{Ep} \right\} \tag{3}$$

$$\sigma_s = P \Big/ \left\{ \frac{Ep}{Es}\ t\,b' + 3A_s \right\} \tag{4}$$

with the corresponding strain given by

$$\epsilon = P \Big/ \left\{ E_p\, t\, b' + 3A_s E_s \right\} \tag{5}$$

while the stiffness is

$$P/\delta = \frac{1}{L} \left\{ E_p\, t\, b' + 3A_s E_s \right\} \tag{6}$$

The above equations apply before initial buckling. Initial skin buckling stress is obtained from[8].

$$\sigma_{crp} = \frac{\pi^2}{tb^2} \left\{ D_{11} \left(\frac{mb}{a}\right)^2 + D_{22} \left(\frac{a}{mb}\right)^2 + 2D_{33} \right\} \tag{7}$$

where m is obtained via

$$m = \frac{a}{b} \sqrt[4]{\frac{D_{22}}{D_{11}}} \tag{8}$$

Note that in Equations (7) and (8) the flexural stiffness terms are obtained from the 'reduced stiffness' matrix.[9]

$$[D^*] = [D] - [B]\,[A]^{-1}\,[B] \tag{9}$$

where the sub-matrices involved form part of the well-known general constitutive anisotropic plate equation.[10]

$$\left\{\begin{matrix} N \\ M \end{matrix}\right\} = \left[\begin{matrix} A & B \\ B & D \end{matrix}\right] \left\{\begin{matrix} \epsilon \\ K \end{matrix}\right\} \tag{10}$$

Use of the reduced stiffness approach has been shown (Reference 9) to give better test-theory correlation for panels with membrane-to-flexure coupling terms in the [B] matrix.

The strain and panel load corresponding to initial buckling may be calculated using Equations (2) and (3) respectively. The test load/inch of panel width is given by

$$N_x = \frac{P}{b'} \tag{11}$$

Following initial buckling, the simplest hypothesis is that the buckled skin takes no further load. Equilibrium then requires that:

$$P = 2b\ t\ \sigma_{crp} + \frac{\sigma_s}{Es} \left\{ tE_p\,(b' - 2b) + 3A_sE_s \right\} \tag{12}$$

The failure load is given by Equation (12) by putting σ_s equal to $\overline{\sigma}_s$ with the failure strain obtained from Equation (2). Equation (12) only gives good results if a reliable value for $\overline{\sigma}_s$ is available.

The predicted panel stiffnesses were all greater than measured stiffnesses by between 10 and 30% (Table 3). This is partly due to eccentricities always present in built-up construction, but more likely reasons are thought to involve fiber collimation and material variability. Panel 10 was considerably less stiff than predicted, due to the presence of the stringer cut-outs (Table 7). Initial buckling mode predictions seem reasonable (Table 4). Predicted strains are all somewhat higher than measured. If the "reduced stiffness" method was not used, even higher predicted strains resulted (e.g. ϵ = 0.00148 instead of 0.00124 for Panel 5). Uncertainties of effective skin thickness and edge restraint influences of the stringers are also acknowledged.

Correlation of results with theory for the aluminum panels (Table 8) was good, reflecting better material uniformity and availability of more firmly established design data[7].

Table 9 and Figure 16 present both strength (σ_{AV}/ρ) and stiffness (E_{EQ}/ρ) data. Panels 1 through four and 10 are about 25% weaker whereas Panel 5 is 18% stronger than the aluminum panels on a strength/density basis. On a stiffness/density basis, the first group of panels demonstrates a 50-130% advantage over aluminum while Panel 5 shows a 200% advantage.

Shear Panels

Correlations (Table 6) were made between measured panel shear stiffnesses and the computed in-plane skin shear stiffnesses. Computed stiffnesses were obtained using measured fiber contents and skin thicknesses. The stringers have a considerable stiffening effect on the skin, although the influence of edge restraints on the test specimen is also likely to be a significant factor.

Three of the four panels tested were analyzed using finite element structural analysis methods. Elastic properties were obtained using measured fiber contents and panel thicknesses. Structural responses were found to be quite complicated involving, in particular, in-plane bending moments, axial stringer loadings, and stringer warping. Results derived from these analyses are also presented in Table 6. Correlation with measurements is within 25%, analytical results being higher in two of three cases.

CONCLUSIONS

Five graphite-fiber, epoxy-resin composite stiffened flat panels were tested in compression. Four composite panels of similar design were tested in shear. In addition, a curved composite panel and two aluminum panels were tested in compression thus involving a total of twelve specimens. Conventional laboratory equipment and testing techniques were found to be adequate. However, the occurrence of room temperature creep in one test shows that loading rate and other time-dependent effects must be studied. High-speed photographic techniques would be desirable to better establish failure modes of compression panels.

Correlations of overall panel stiffnesses, initial buckling modes and strains with measured values were reasonable. The effect of material variability, particularly laminate thickness, was found to be significant. Better fabrication and process controls, together with improved fiber treatments, should enable more accurate response predictions and ultimately permit higher strength levels to be achieved. Valuable insights were gained with respect to design of stiffened panels where strength and stiffness tradeoffs between shear and compression loading requirements are involved.

There is need for further analytical work in developing post-buckling analyses for anisotropic plates, stiffened panels, and shells. Effects of stringer restraint on the skin buckling must also be investigated. It may be eventually possible to allow initial skin buckling below limit load which would result in additional weight savings for nonoptimum composite structures.

The compression panels demonstrated a very large weight-stiffness advantage over aluminum construction-up to 200%. Stiffness critical structures such as large slender fuselages, long columns, wing panels, flaps, and doors subjected to buckling, flutter, or displacement limitations should be advantageous application areas for graphite fiber reinforced composites.

The compression strength potential of graphite composite structures was demonstrated in limited testing of untreated Thornel 40 stringer elements and in the test of a treated Thornel 50 stiffened compression panel. Considerable work is yet required to establish reliable material design data and fabrication processes. Vigorous efforts have been undertaken to improve the basic fiber to matrix adhesive bonding which is associated with composite strength properties. Environmental and service life data on graphite composites are also needed.

ACKNOWLEDGEMENTS

Acknowledgements to the following Bell Aerosystems personnel are made: W. H. Dukes, Chief Engineer, Structural Systems Dept., for overall technical guidance; F. M. Anthony, Assistant Chief Engineer and ARPA Program Supervisor; R.A.C. Ross, Computer Programming; G.A. Spiering, Mechanical Testing, R.A. Willard, Jr., and G.T. Climes, Manufacturing Engineering Department.

The authors also thank Dr. G. B. Spence, A. A. Pallozzi and O. L. Blakslee of Union Carbide Corporation for their contributions in technical guidance, specimen fabrication, and suggestions regarding test methods, and express their gratitude to Prof. T. P. Kicher and J. Mandell of Case Western Reserve University for helpful discussion on analysis methods.

REFERENCES

1. Blakslee, O.L., Pallozzi, A.A., Doig, W.A., Spence, G.B., and Hanley, D.P., "Fabrication, Testing, and Design Studies with 'Thornel' Graphite-Fiber, Epoxy-Resin Composites," 12th National SAMPE Symposion, Anaheim, California, October 10-12, 1967.

2. Hanley, D.P., and Cross, S.L., "Studies Related to the Acoustic Fatigue Resistance of Advanced Composites," 12th National SAMPE Symposium, Anaheim, California, October 10-12, 1967.

3. Anthony, F.M., and Hanley, D.P., "Design Procedures for a Graphite Fiber Composite Structure," ASME Winter Annual Meeting, Pittsburgh, Pennsylvania, November 1967.

4. Spence, G.B., "Graphite Fiber Composite Materials," ASME Winter Annual Meeting, Pittsburgh, Pennsylvania, November, 1967.

5. Dukes, W.H., and Krivetsky, A., "The Application of Graphite Fiber Composites to Airframe Structures," SAE Air Transportation Meeting, New York, N.Y., April 29-May 2, 1968.

6. Union Carbide Corporation Carbon Products Division in Association with Case Western Reserve University and Bell Aerosystems Company, a Textron Company, "Integrated Research on Carbon Composite Materials," AFML-TR-66-310, Part II (December 1967).

7. Anon., "Bell Aerosystems Company Structures Manual"

8. Hearmon, R.F.S., "An Introduction to Applied Anisotropic Elasticity," equation 7.8.7, Oxford University Press, Oxford, England, 1961.

9. Mandell, J.F., "An Experimental Study of the Buckling of Anisotropic Plates," M.S. Thesis, Case Western Reserve University, June 1968.

10. Tsai, S.W., "Strength Characteristics of Composite Materials," NASA CR-224, equation 1, April 1965.

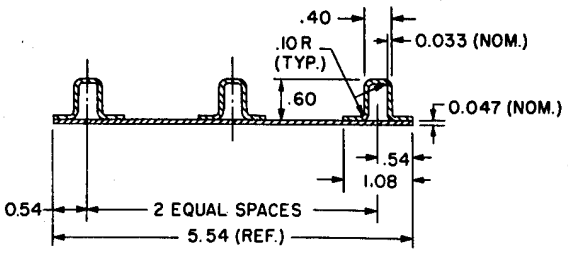

NOTES:

1. PANELS WERE VARIOUS LENGTHS – SEE TABLES
2. POTTING WAS 6.5-IN. WIDE x 2.0-IN. DEEP x 1.2-IN. WIDE. (CENTERED ON PANEL CENTROID)

FIGURE 1. COMPRESSION PANEL GEOMETRY

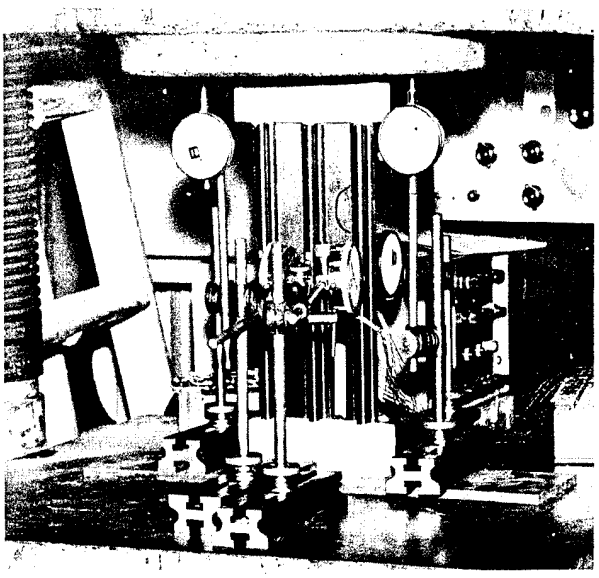

FIGURE 4. COMPRESSION PANEL TEST SETUP (PANEL 1)

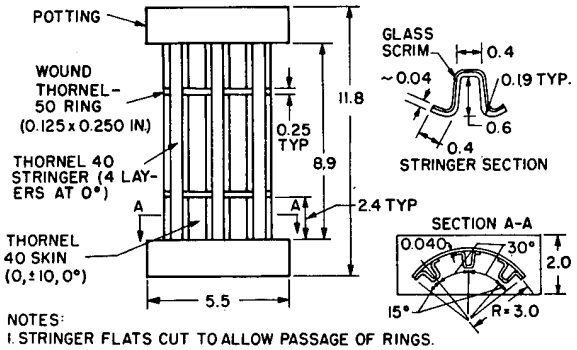

NOTES:

1. STRINGER FLATS CUT TO ALLOW PASSAGE OF RINGS.
2. STRINGERS HAVE GLASS SCRIM CLOTH OVER OUTER LAYERS.

FIGURE 2. CURVED COMPRESSION PANEL (PANEL 10)

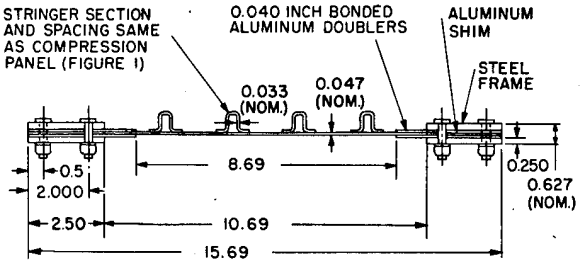

NOTE:

1. UNSUPPORTED PANEL AREA WAS SQUARE.
2. 0.12-INCH GAP BETWEEN STRINGER ENDS AND DOUBLERS.

FIGURE 5. SHEAR PANEL GEOMETRY

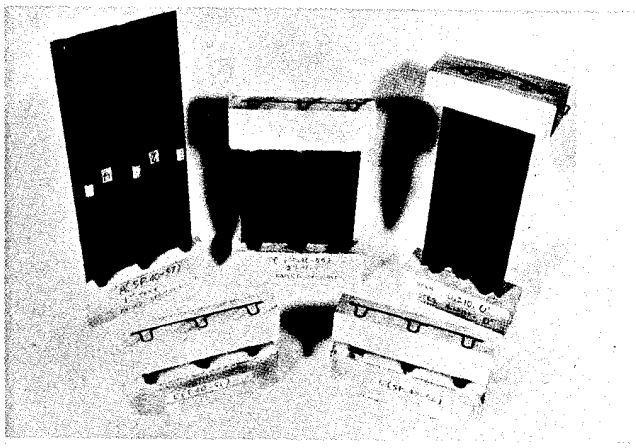

FIGURE 3. GROUP OF COMPRESSION PANELS

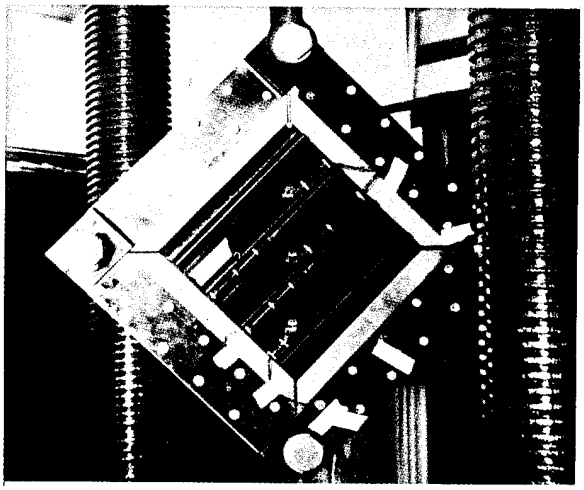

FIGURE 6. SHEAR PANEL TEST SETUP (PANEL 6)

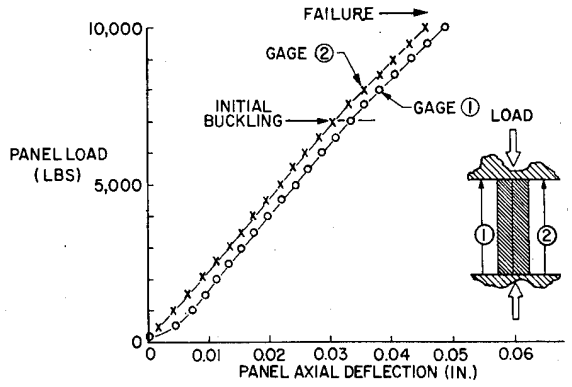

FIGURE 7. TYPICAL RESULT-COMPRESSION OVERALL STIFFNESS (PANEL 4)

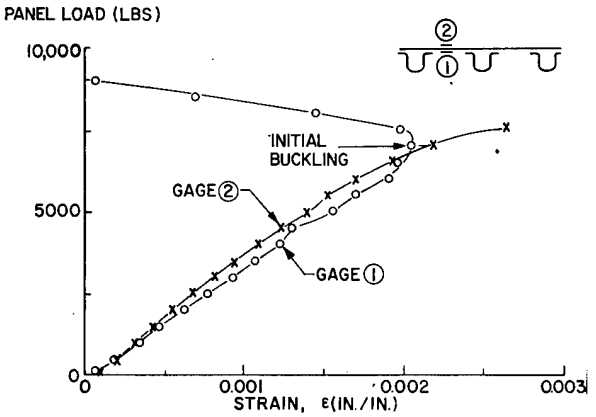

FIGURE 8. TYPICAL RESULT-COMPRESSION PANEL INITIAL BUCKLING (PANEL 4)

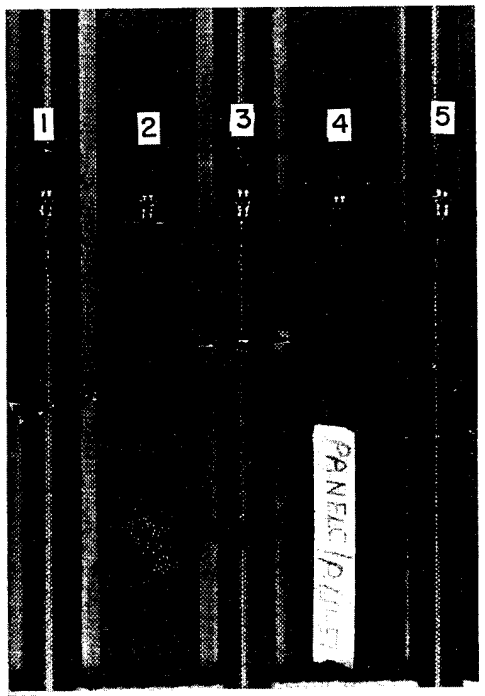

FIGURE 9. COMPRESSION PANEL FAILURE-ORTHOGONAL STRINGERS (PANEL 1)

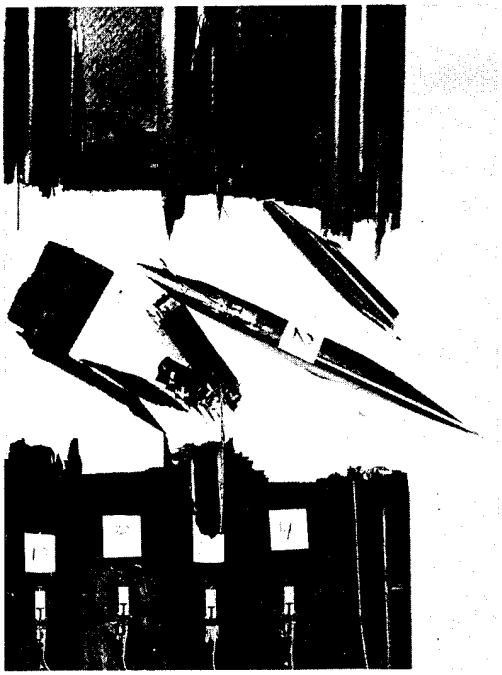

FIGURE 10. COMPRESSION PANEL FAILURE - ±10° STRINGERS (PANEL 5)

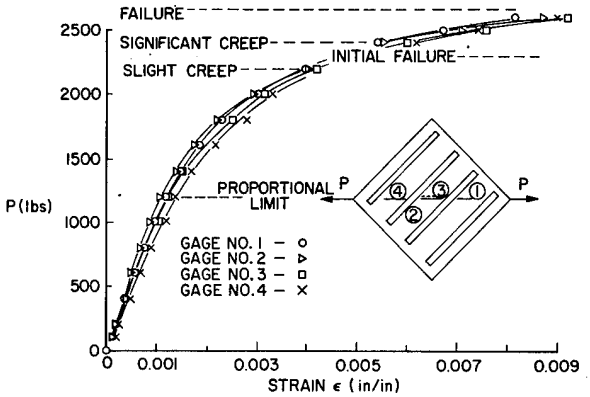

FIGURE 11. TYPICAL RESULTS - SHEAR PANEL STRAINS (PANEL 6)

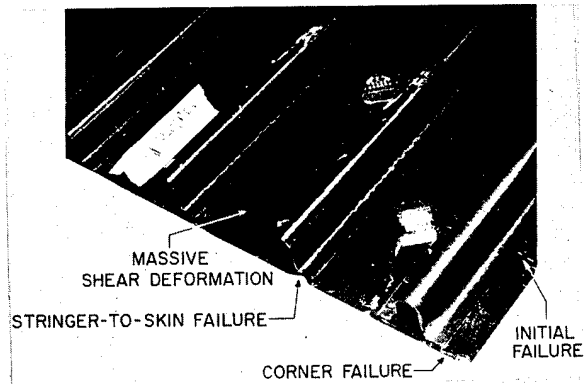

FIGURE 12. SHEAR PANEL FAILURE - LOCAL FAILURES (PANEL 6)

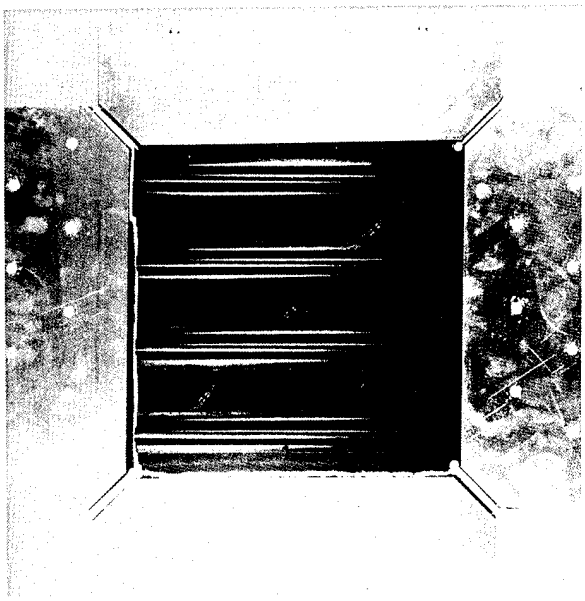

FIGURE 13. SHEAR PANEL FAILURE - EDGE FAILURES (PANEL 9)

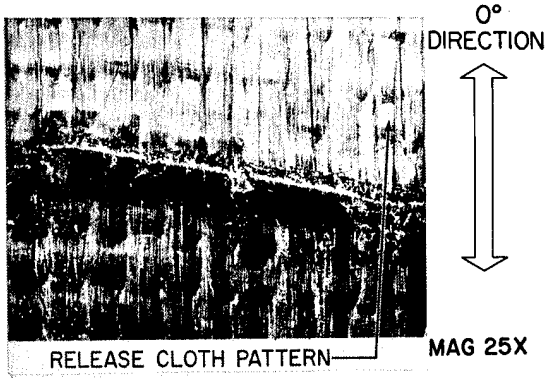

FIGURE 14. COMPRESSION PANEL FAILURE DETAIL; ORTHOGONAL SKIN (PANEL 1)

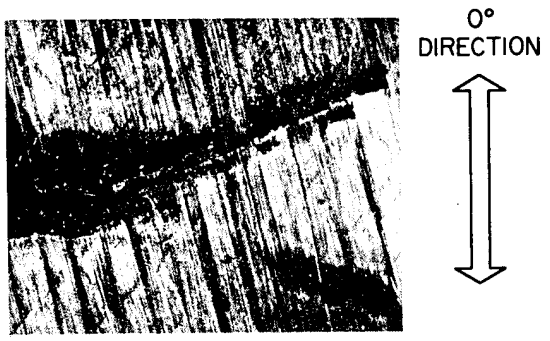

FIGURE 15. COMPRESSION PANEL FAILURE DETAIL; 10° STRINGER FLAT (PANEL 3)

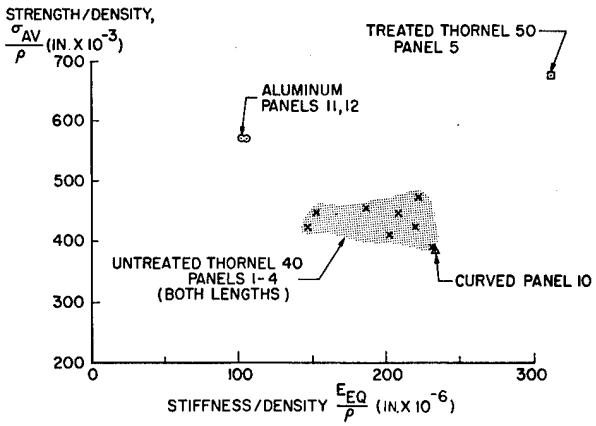

FIGURE 16. SPECIFIC STRENGTH AND STIFFNESS OF COMPRESSION ELEMENTS

TABLE 1. COMPRESSION PANEL CHARACTERISTICS

PANEL	LAYUPS		LAMINATE CHARACTERISTICS			
			SKIN		STRINGERS	
	SKIN	STRINGERS	t (in.)	V_F (%)	t (in.)	V_F (%)
1	0,90,90,0^o	90,0,0,90^o	0.039	54.6	0.038	59.3
2	90,0,0,90	90,0,0,90	0.042	51.0	0.041	55.0
3	90,±25,90	∓10,±10	0.037	55.6	0.039	57.0
4	90,±25,90	90,0,0,90	0.046	42.0	0.039	56.3
5	90,±15,90	±10,∓10	0.035	53.0	0.038	50.3

NOTES: (1) PANELS 1 - 4 ARE UNTREATED THORNEL - 40 FIBER; PANEL 5, TREATED THORNEL - 50

(2) 0^o DIRECTION IS PARALLEL TO THE STRINGERS

TABLE 2. SHEAR PANEL CHARACTERISTICS

PANEL	LAYUPS		LAMINATE CHARACTERISTICS			
			SKIN		STRINGERS	
	SKIN	STRINGERS	t (in.)	V_F (%)	t (in.)	V_F (%)
6	0, 90, 90, 0^o	90, 0, 0, 90^o	0.039	55.9	0.034	54.3
7	90, ±25, 90	90, 0, 0, 90	0.036	55.8	0.040	55.3
8	90, ±25, 90	±10, ∓ 10	0.042	52.0	0.039	58.5
9	90, ±15, 90	± 10, ∓10	0.038	50.5	0.036	50.5

NOTES: (1) PANELS 6-8 ARE UNTREATED THORNEL-40 FIBER; PANEL 9, TREATED THORNEL-50
(2) 0^o DIRECTION IS PARALLEL TO THE STRINGERS

TABLE 3. COMPRESSION PANEL OVERALL STIFFNESSES

PANEL	$\frac{P}{\delta}$ (lb/in. x 10^{-6})			
	FULL-LENGTH PANELS (L=16 in.)		CUT-DOWN PANELS (L≈10 in.)	
	MEASURED	PREDICTED	MEASURED	PREDICTED
1	0.292	0.330	0.535	0.574
2	0.282	0.334	0.507	0.558
3	0.307	0.404	0.532	0.673
4	0.226	0.270	0.350	0.405
5	0.420	0.490	-	-

NOTE: L IS THE OVERALL PANEL LENGTH (INCLUDING POTTING)

TABLE 4. COMPRESSION PANEL INITIAL BUCKLING CORRELATION

PANEL	FULL-LENGTH PANELS (a ≃ 12 in.)				CUT-DOWN PANELS (a ≃ 5.5 in.)			
	MODE (m)		STRAIN ϵ (in./in.)		MODE (m)		STRAIN ϵ (in./in.)	
	M	P	M	P	M	P	M	P
1	8	7	0.00134	0.00147	3 or 4	3	0.00160	0.00164
2	16	16	0.00141	0.00188	7	8	0.00156	0.00193
3	~12	19	0.00158	0.00171	10 or 11	8	0.00179	0.00217
4	16	18	0.00193	0.00274	11	10	0.00175	0.00278
5	17	18	0.00097	0.00124	-	-	-	-

NOTES: (1) a IS THE FREE PANEL LENGTH (EXCLUDING POTTING)
(2) M = MEASURED; P = PREDICTED

TABLE 5. COMPRESSION PANEL STRENGTHS

PANEL	INITIAL BUCKLING N_x (lb/in.)		ULTIMATE PANEL STRENGTHS				
			L=16 in.			L ≃ 10 in.	L ≃ 4 in.
	L=16 in.	L ≃ 10 in.	N_x (lb/in.)	σ_s (psi)	$\bar{\sigma}_s$ (psi)	N_x (lb/in.)	N_x (lb/in.)
1	1,110	1,350	1,800	20,900	-	1,720	2,610
2	1,170	990	1,980	24,100	-	1,790	1,820
3	1,490	1,350	1,890	32,000	25,100	1,560	-
4	1,170	990	1,880	25,500	24,500	1,990	-
5	1,080	-	2,620	44,600	48,000	-	-

NOTES: (1) L IS THE OVERALL PANEL LENGTH (INCLUDING POTTING).
(2) REQUIRED INITIAL BUCKLING STRENGTH 1,200 lb/in.
(3) REQUIRED ULTIMATE STRENGTH 1,800 lb/in.
(4) STRINGER STRENGTHS $\bar{\sigma}_s$ DETERMINED BY SEPARATE COMPRESSION TEST.

TABLE 6. SHEAR PANEL RESULTS

PANEL	PROPORTIONAL LIMIT (lb/in.)	ULTIMATE STRENGTH (lb/in.)	SHEAR STIFFNESSES, G (psi x 10^{-6})		
			PANEL (MEASURED)	PANEL (FINITE ELEMENT METHOD)	SKIN ONLY (PREDICTED)
6	104	240	1.10	1.47	0.63
7	302	400	3.49	4.61	2.14
8	215	430	5.43	4.44	1.99
9	129	416	1.74		1.32

NOTES: (1) REQUIRED LIMIT STRENGTH 120 lb/in.
(2) REQUIRED ULTIMATE STRENGTH 180 lb/in.

TABLE 7. CURVED COMPRESSION PANEL RESULTS (PANEL 10)

a.) PANEL TEST

P/δ (lb/in. x 10^{-6})		ULTIMATE STRENGTH			
MEASURED	PREDICTED	LOAD (lb)	LOADING, N_x (lb/in.)	ESTIMATED STRINGER STRESS (psi)	ESTIMATED SKIN STRESS (psi)
0.480	0.807	9,400	2,000	28,000	26,800

NOTES: (1) STIFFNESS PREDICTED USING GROSS STRINGER AREA
(2) STRESSES ESTIMATED USING NET STRINGER AREA

b.) STRINGER TESTS
(SHORT SPECIMENS CUT FROM CYLINDER)

SPECIMEN	FAILURE STRESS (psi)
1	78,000
2	91,200
3	72,000

TABLE 8. ALUMINUM COMPRESSION PANEL RESULTS

PANEL	$\frac{P}{\delta}$ (lb/in. x 10^{-6})		INITIAL BUCKLING						ULTIMATE STRENGTH N_X (lb/in.)	
			MODE (m)		STRAIN, ϵ (in./in.)		LOADING, N_x (lb/in.)			
	M	P	M	P	M	P	M	P	M	P
11	0.530	0.544	5	5	0.00400	0.00439	2,980	3,450	4,270	4,450
12	0.545	0.544	5	5	0.00380	0.00439	2,805	3,450	4,270	4,450

NOTES: (1) PANEL OVERALL LENGTH (INCLUDING POTTING)= 8.0 IN.
(2) PANEL FREE LENGTH (EXCLUDING POTTING)= 6.0 IN.
(3) M = MEASURED, P = PREDICTED

TABLE 9. ALUMINUM AND GRAPHITE COMPOSITE COMPARISON

COMPRESSION PANEL	MATERIAL	COMPRESSIVE STRENGTH			COMPRESSIVE STIFFNESS	
		$\frac{W}{b}$ (pci)	$\frac{N_x}{b}$ (psi)	$\frac{\sigma_{av}}{\rho}$ (in. x 10^{-3})	E_{eq} (psi x 10^{-6})	$\frac{E_{eq}}{\rho}$ (in. x 10^{-6})
ALUMINUM (AVERAGE)	7075-T6	0.00142	771	570	10.4	104
BEST GRAPHITE (PANEL 5)	THORNEL-50	0.00070	472	671	16.2	312